PROSPECTS FOR THE USE OF PATHOLOGICAL BIOMINERALIZATION IN THE DIAGNOSIS OF OVARIAN CANCER

Ruslana Chyzhma[1]
Roman Moskalenko[2]

Abstract. Ovarian cancer is one of the most common causes of death in the female population. Among malignant tumors, ovarian cancer ranks fourth after neoplasms of the body, cervix, and mammary gland. High mortality rates in malignant ovarian neoplasms are primarily due to the asymptomatic course, the ineffectiveness of screening diagnostic methods, and the progression of the tumor process. One of the clinical and morphological features of ovarian cancer is pathological biomineralization. *The purpose of the work* is to establish the morphological features and phase composition of pathological biominerals. Also to investigate the potential diagnostic value of mineral formations of ovarian cancer. We have analyzed 60 samples of ovarian cancer by histopathology (hematoxylin-eosin and von Kossa staining), immunohistochemistry, scanning electron microscopy with EDX and transmission electron microscopy. *Results*. We detected hyperechoic formations of a rounded shape with smooth edges and precise contours during the ultrasound diagnosis of ovarian cancer. The size ranged from 2 to 5 mm. Histological analysis demonstrated the presence of psammoma bodies (Pbs) in the tumor tissue of the ovary with a variation in the amount from 1 to 200 units. PBs were mainly localized at the base of papillary growths of ovarian serous carcinoma and tumor tissue detritus. The sizes of these formations varied from 12.6 to 493.7 μm. Psammoma bodies and their fragments in the tumor tissue were stained black with von Kossa staining. This indicates the presence of calcium phosphate salts in the composition of these bodies. Immunohistochemical

---

[1] Ph.D. Student at the Department of Pathology,
Academic and Research Medical Institute, Sumy State University, Ukraine
[2] MD, Professor, Associate Professor at the Department of Pathology,
Academic and Research Medical Institute, Sumy State University, Ukraine

examination of ovarian cancer tissue demonstrated the accumulation of OPN and OC on the surface of mineral formations. This indicates the presence of hydroxyapatite and proteins in the structural composition of PBs. Scanning electron microscopy established that the calcifications have different sizes, rounded shapes, and fragile structures. The main lines of Ca and P were present in the EDX spectra. Their intensity ratio reflects the characteristic features of hydroxyapatite $Ca_{10}(PO_4)_6(OH)_2$. Transmission electron microscopy demonstrated the poly- and monodispersity of apatite crystals. The electron diffraction (ED) pattern indicates the polycrystalline nature of these mineral inclusions. Crystalline particles ranged in size from 5 to 15 nm to 40 to 50 nm, which illustrates the polydisperse morphology of nanosized crystals of the pathological deposit. Therefore, studying the structure, physicochemical, and phase composition of ovarian cancer calcifications, and their imaging features is essential because of the possible practical application of this pathological phenomenon for the early diagnosis of ovarian cancer and other malignant neoplasms with biomineralization. The structural properties of biomineral deposits of tumor tissue make it possible to increase the accuracy of early diagnosis, and the informativeness of the final result at the pre-and postoperative stages, which can improve the prognosis and preserve the quality of life of patients.

1. Introduction

Ovarian cancer leads to the general structure of oncological morbidity of the female reproductive system [1]. Morbidity and mortality rates show an increasing trend every year [1; 2]. Among malignant tumors, ovarian cancer ranks fourth after neoplasms of the body, cervix, and mammary gland [2]. Although ovarian cancer has a lower prevalence rate compared to breast cancer, mortality in this pathology is three times higher [2; 3].

High mortality rates in malignant ovarian neoplasms are primarily due to the asymptomatic course, the ineffectiveness of screening diagnostic methods, and the progression of the tumor process [3]. It has been established that ovarian tumors are diagnosed at the late stages (III-IV) of the disease. Only isolated cases are diagnosed at the early stages (I-II) of development [3; 4]. It is characterized by a five-year survival rate that reaches 92% and 28% for stages I-II and III-IV, respectively [2–4]. Approximately 80% of women with late-stage ovarian cancer experience progression or recurrence

of the tumor process [5]. This leads to a decrease in indicators of work capacity and quality of life of the female population, which constitutes a medical and social problem on a global scale [6; 7]. High mortality rates are due to difficulties in early diagnosis. Ovarian cancer is often an incidental finding during the examination due to complications or other pathology [8].

The highest incidence rate is observed in the industrialized countries of the world. In particular, in North America, Central, and Northern Europe the rate exceeds 8 cases per 100 000 population [2]. At the same time, the lowest rate is observed in Africa and Asia, amounting to < 3 cases per 100,000 population [2; 3]. In Ukraine, the incidence rate is 11.3 cases per 100 000 female population. In particular, the Sumy region is characterized by a high level of malignant neoplasms of the ovaries (12.5 per 100 000 female population) [1].

It should be noted that the results of ovarian cancer treatment depend on many factors. Such as the stage of the disease, the type of tumor process, histogenesis, as well as the degree of differentiation. Thus, this once again indicates the importance of early diagnosis of malignant neoplasms of the ovaries [9–11].

2. Etiology and pathogenesis

The high prevalence of ovarian neoplasms is associated with the influence of such factors as women's age (45-70 years), early menarche and late postmenopausal period. This is characterized by an increase in the number of ovulatory cycles and an increase in hypothalamic-pituitary activity. A significant role in the development of ovarian tumors is played by genetic predisposition and gynecological diseases, including pelvic inflammatory disease, endometriosis, polycystic ovary syndrome [12].

The hypothesis of "continuous ovulation" suggests that the number of ovulatory cycles increases the rate of cell division, which is directly related to the restoration of the surface epithelium after each ovulatory cycle, thereby increasing the risk of spontaneous mutations [13].

The genetic factor is characterized by mutations in genes such as BRCA, KRAS, BRAF, ERBB2, CTNNB1, PTEN, PIK3CA, ARID1A, PPP2R1A, and TP53 [14]. Women with a hereditary history of ovarian cancer usually have mutations in BRCA1 and BRCA2, which are predictors of the risk of developing this pathology [15]. In addition, BRCA1 and BRCA2 account

for approximately 15% of all ovarian malignancies. BRCA1 mutation carriers have been found to have a 40-50% risk of developing ovarian tumors during their lifetime. At the same time, BRCA2 mutation carriers have a 20-30% risk of developing this pathology [16].

Also, some factors contribute to reducing the risk of this pathology. These include pregnancy, lactation, and taking oral contraceptives, which reduces the risk of developing this pathology by 7% [17]. It has been established that women who have given birth have a 30-60% lower risk than women who have not given birth [18; 19]. Each subsequent full-term pregnancy reduces the risk by approximately 15% [20; 21].

Ovarian cancer symptoms are non-specific. Therefore, it is quite easy to miss them and confuse them with other pathological processes. This complicates diagnostic possibilities in the early stages [22; 23]. Specific clinical signs appear in the later stages of the disease (III-IV) and include a combination of such symptoms as abdominal distension, nausea, early satiety, violation of the act of defecation and urination, manifestations of ascites, as well as back pain, rapid fatigue, and weight loss [24].

In addition, stage III and IV ovarian cancer is characterized by metastatic lesions [25]. One of the features of ovarian cancer is the unique behavior of the metastatic process of this disease [26]. After all, it is noticeably different from the classic model of hematogenous metastasis, which is characteristic of most types of cancer of various localizations [27].

This model includes several stages of intra- and extravasation and only after that metastases are formed in other organs [28]. At the same time, ovarian tumors metastasize according to the passive mechanism. The tumor cells are separated from the primary neoplasm of the ovary in the form of single cells or their clusters. Due to the physiological movement of peritoneal fluid, they circulate to the peritoneum and omentum, where they form tumor implants [29]. An interesting fact about ovarian cancer is that these implants penetrate the layers of mesothelial cells, while rarely reaching the deep layers of the peritoneum [30].

Tumor cells undergo an epithelial-to-mesenchymal transformation before detaching and starting their metastatic journey [31]. This weakens the intercellular connections of tumor cells and facilitates the attachment of epithelial cells to the basement membrane [32]. Transformed cells resemble fibroblasts, acquiring an invasive phenotype and actively

proliferating [33]. Ovarian tumor cells change from a mesenchymal to an epithelial phenotype after the construction of a metastatic colony in the tissue of the omentum and peritoneum [34]. This allows them to maintain rapid growth and respond to paracrine growth factors [35].

3. Features of pathological biomineralization in malignant neoplasms of the ovaries

About 90% of primary ovarian neoplasias are epithelial-stromal, of which 70% are ovarian serous adenocarcinomas. They are divided into low-grade and high-grade tumors [35; 36]. One of the clinical and morphological features of serous adenocarcinomas is pathological biomineralization. In 8% of cases, pathological biomineralization is detected by computer tomography. Histologically, the frequency of microcalcifications in low-grade and high-grade serous carcinomas reaches 100% and 50%, respectively [36]. Pathological crystalline inclusions begin to develop in the early stages of carcinogenesis. The presence of biominerals contributes to the growth of five-year survival rates for ovarian tumors to 50% [37].

The process of pathological biomineralization in ovarian tissue is represented by psammoma bodies (PBs), calcification of the capsule, and stroma of tumor nodes [38; 39]. It has been established that calcium deposition occurs in degenerated and necrotic tissue with a normal level of calcium in blood serum or the absence of disturbances in calcium metabolism in the body [40]. PBs have lamellar calcified structures, which are presented in the form of concentric circles [41; 42]. The presence of PBs is a pathognomonic sign in the diagnosis of malignant neoplasms of the ovaries and is visualized by instrumental diagnostic methods, such as ultrasound diagnostics (US), computerized tomography (CT), and magnetic resonance imaging (MRI), as well as by histological examination [43; 44].

Most systems of the human body are in ionic equilibrium with blood. Blood is a metastable solution of Ca^{2+} and PO_4^{3-} [45]. Mineralization inhibitors are present in the blood, which stabilize the metastable solution to that these pathological biominerals are not formed throughout the body [46]. Matrix vesicles reduce the level of calcification inhibitors during normal biomineralization of skeletal tissue [47]. As soon as the cells begin to produce matrix vesicles, the formation of pathological biominerals increases in weak areas, namely, areas of inflammation, necrotic changes,

and the tumor process [48]. Matrix vesicles stimulate a signaling cascade similar to the formation of normal skeletal tissue. At the same time, one of the consequences of this mechanism is the formation of matrix vesicles. This indicates the continuity of their release and activation of the signaling cascade [49]. Matrix vesicles and mitochondria usually initiate calcification through the interaction of phosphatase enzymes with calcium-binding phospholipids [50].

Also, one of the main components in the formation of hard tissues is alkaline phosphatase, which is highly expressed in mineralized cells of soft tissues [51]. This enzyme performs its function by increasing the local concentration of inorganic phosphate (stimulator of mineralization). Also, alkaline phosphatase helps to reduce the concentration of extracellular pyrophosphate, thereby inhibiting mineral formation [52].

Some studies have shown that psammoma bodies can create a barrier to the spread of neoplastic cells and even lead to their death. This promotes tumor regression at an early stage of development [53]. This is confirmed by the results of radiological control of the treatment of malignant tumors of the ovaries. Calcification is more common in highly differentiated tumors with low malignancy, and after treatment, the presence of biomineralization in peritoneal metastases increases to 16% [54]. In the later stages of development, calcification may be the result of biological changes in the tumor and indicate progression and an unfavorable prognosis [55].

It was established by electron microscopy that the formation of PBs occurs in histiocytes of the stroma and neoplastic cells. Also, some studies show that ovarian cancer calcifications are found mainly in the stroma of the tumor and not in the epithelium [56; 57]. At the same time, regardless of the location of these calcifications, their presence contributes to the growth of five-year survival rates to 50% [58].

There is also a theory that the process of calcification in ovarian neoplasms is similar to metastatic calcification, which is characterized by hypercalcemia and formation in normal tissues [59]. However, there is an opinion that this process is related to the secretion of collagen by tumor cells or is provoked by the combined effect of such hormones as prolactin, estradiol, estrone, somatotropic hormone, testosterone, and human chorionic gonadotropin [60; 61].

The mechanism of the development of vascular calcification in ovarian neoplasms is characterized by the expression of transcription factors and bone matrix proteins. Thus, replacing the contractile function of vascular smooth muscles with a calcifying one [62]. This indicates the similarity between the mechanisms of mineralization and osteogenesis.

The study of the chemical composition of pathological biominerals is an important step in understanding the mechanism of development and their direct role in the early diagnosis or prognosis of this disease. It was established that the composition of PBs includes such inorganic elements as Al (aluminum), Cd (cadmium), K (potassium), Co (cobalt), Cr (chromium), Fe (iron), Zn (zinc), and Cu (copper) [63]. Energy dispersive X-ray spectroscopy showed that the composition of PT includes Ca (calcium), P (phosphorus), Mg (magnesium), and Na (sodium) [64; 65].

One of the molecular bases of pathological biomineralization in ovarian neoplasms is the presence of such calcification biomarkers as BMP-2, Runx2, Osterix, and OPN [66].

BMP-2 is a member of the BMP (bone morphogenetic protein) family of proteins and has osteoinductive activity, such as direct enhancement of cell calcification and modeling of osteogenesis pathways [67]. Through the BMP/Smad pathways, signals are transmitted to regulate the synthesis of osteogenic factors, including OPN [68]. OPN inhibits bone calcification, which in turn controls biomineralization. The OPN protein is secreted by macrophages, contributing to the deposition of calcium phosphate and the formation of psammoma bodies [69; 70]. OPN is overexpressed by tumor cells. By activating signaling pathways that provide regulation of HIF-1α, it affects angiogenesis, tumor cell adhesion, proliferation, and metastasis [71]. The transcription factors Runx2 and Osterix provide OPN control. Also, they have a necessary role in the differentiation and maturation of osteoblasts, regulating their proliferation [72]. Runx2 takes a direct role in early osteogenic differentiation and Osterix in the late stages of osteogenic differentiation. Therefore, the appearance of these biomarkers of mineralization in ovarian neoplasms indicates the process of osteogenesis of ovarian tumors [73].

However, there is a whole set of unsolved problems associated with the complexity of understanding the processes of formation of these

biominerals. Also, their role in the early diagnosis of malignant neoplasms of the ovaries.

The purpose of the work is to establish the morphological features and phase composition of pathological biominerals. Also to investigate the potential diagnostic value of mineral formations of ovarian cancer.

4. Materials and methods

The conduct of the study was approved by the ethics committee of the Academic and Research Medical Institute of Sumy State University (protocol No. 1/12, December 8, 2022). All studies were performed by the requirements of the Law of Ukraine "On Medicinal Products", 1996, Art. 7, 8, 12, ICH GCP (2008), GLP (2002), by the requirements and standard provisions of the order of the Ministry of Health of Ukraine No. 690 dated September 23, 2009. "On approval of the procedure for conducting clinical trials of medicinal products and examination of materials of clinical trials and standard regulations of the commission on ethics".

30 samples of malignant ovarian neoplasms with signs of calcification (group 1) and 30 samples of malignant ovarian neoplasms without signs of calcification (group 2) were selected for the study. All cases of ovarian cancer were studied clinically, instrumentally (ultrasound diagnosis), and morphologically (represented by surgical material after oophorectomy and panhysterectomy). All patients underwent surgical treatment in the gynecological departments of SMKL № 1 and SOKOD.

Detection of pathological biominerals

Calcifications with a diameter of more than 0.5 mm were detected during the macroscopic diagnosis of tumor tissue samples.

Pathological biomineral formations with a diameter of less than 0.5 mm were investigated by histological examination and scanning electron microscopy from histological sections of tumor tissue.

Ultrasound

Ultrasound diagnostic examination of women with ovarian diseases was carried out using a Toshiba Aplio MX device with a 6-12 MHz linear multifrequency sensor (Japan) based on the private clinic "Floris".

Histology and histochemistry

The tissue material of ovarian tumors was fixed in a neutral (buffered) 4% formaldehyde solution for 24 hours. Histological blocks were prepared

195

after dehydration and paraffin embedding. Serial sections of 4 μm thickness were made using a Shandon Finesse 325 rotary microtome (Thermo Scientific). After deparaffinization and dehydration (xylene and ethanol), histological sections were stained with hematoxylin and eosin.

Histological sections of tumor tissue were treated with a 5% aqueous solution of silver nitrate (Von Kossa method) under the direct light of a 60 W lamp for 60 minutes to determine calcium deposition. The tissue samples were then treated with sodium thiosulfate (5% aqueous solution). Nuclei were stained with an aqueous solution of fast nuclear red fast for 5 minutes (1:1000).

During the microscopic examination, the following characteristics of ovarian cancer were taken into account: histological type of structure (according to the WHO classification), type of calcification, presence of metastases, and nature of vascularization.

Immunohistochemistry

Deparaffin sections were subjected to temperature unmasking of the antigen in 0.1 M citrate buffer (pH 6.0) at a temperature of 95–98°C (Thermo Scientific, USA). Conducting and visualization of the immunohistochemical reaction was carried out using the detection system "UltraVision Quanto Detection System HRP Polymer" (Thermo Scientific, USA) and "DAB Quanto Detection System" (Thermo Scientific, USA). The following primary antibodies were used: OPN (Anti-Osteopontin antibody, ab 37807, Abcam, Cambridge, Great Britain), OC (Anti-Amyloid Fibrils, ab2286, Merck, Germany). Nuclei were contrasted with Mayer's hematoxylin.

Morphometric analysis

The evaluation of morphometric data was carried out using the software "Panoramic Viewer" (3DHistech, Hungary) and "Zen 2.0" (Carl Zeiss, Germany). The positive reaction of cells was counted in the field of view of 1000 μm. At least 6 fields of each sample were analyzed.

Photographs were obtained using a digital imaging system "Zen 2.0" (Carl Zeiss, Germany) and "Panoramic Viewer" (3DHistech, Hungary). + SEO Scan Lab 2.0

Physico-chemical research methods

The study of biominerals using the methods of applied materials science was carried out in the laboratory of the Institute of Applied Physics of the

National Academy of Sciences of Ukraine (head – Candidate of Physical and Mathematical Sciences Sergiy Danylchenko).

The mineral component of macroscopic calcifications was separated from soft tissues by heat treatment in an electric furnace at a temperature of 200°C for 1 hour. This contributed to the destruction of the organic part of the calcification and the removal of water residues while preserving the structure of the crystallite. The material was also treated at 900°C for 1 hour, which allowed to complete separate the organic and non-acrylic components of biominerals.

Scanning electron microscopy with EDX

From the prepared paraffin block of tissue, histological sections with a thickness of 10-12 μm were made, which were placed on a stage made of spectrally pure graphite. The sections were kept in a thermostat at a temperature of 60°C for 30 minutes. Then the histological sections were deparaffinized using xylene and ethyl alcohol. The prepared preparations were examined on an SEO-SEM Inspect S50-B scanning microscope (Ukraine) with an AZtecOne energy dispersive spectrometer with an X-MaxN20 detector (Oxford Instruments plc, Abingdon, UK). Processing of EDX spectra was carried out by standard software of the microanalysis system.

Transmission electron microscopy

Transmission electron microscopy (TEM) by electron diffraction (ED) was performed on a TEM-125K microscope (SELMI, Ukraine). The mineralized tissue in the form of powder was treated with ultrasound in distilled water using the UZDN-A unit (SELMI, Ukraine). The specific power of the installation is 15-20 W/cm^2 at the emitter frequency of 22 kHz. The obtained suspension (several drops) was applied to the vertically upward ultrasonic emitter UZDN-A and sprayed for 2-3 seconds, changing the power of the installation. The sprayed aerosol was caught on a thin carbon film (10-20 nm) located on the copper grid of the sample holder. ED images and photomicrographs were obtained at a voltage of U(injector) = 90 kV.

Statistical analysis

The results of the morphometric and immunohistochemical study were checked for normal distribution using the Shapiro-Wilk test. The Mann-Whitney test was used to assess the statistical significance of non-normal distribution.

197

Data samples that corresponded to a normal distribution were compared using the parametric Student's t-test.

5. Results

Ultrasound

During the ultrasound diagnosis of ovarian cancer were found single hyperechoic formations of a rounded shape with smooth edges and clear contours, homogeneous in echo structure, and with the absence of acoustic shadows. These formations ranged in size from 2 to 5 mm and were characterized by an avascular type of vascular pattern in the surrounding tissues.

Histology

The tissue of ovarian serous carcinoma is histologically characterized by micro- and macropapillary growths, single cells, and randomly formed small nests of cells with stroma infiltration. Tumor cells are monomorphic, small in size, and have moderate nuclear atypia and pronounced nucleoli. Individual samples of serous carcinomas are represented by solid masses with slit-like lumens, tumor cells with large, hyperchromic, pleomorphic nuclei of a chimeric configuration. Multinucleated cells with eosinophilic nuclei also occur in the tumor tissue. Necrotic changes are absent in most samples of serous carcinoma.

All selected samples contained pathological biomineral formations in the form of psammoma bodies (PBs). PBs are represented by concentric calcified structures and their irregularly shaped fragments. Debris is formed due to mechanical damage by a microtome blade during the stages of his technical preparation of micro preparations. Point mineral deposits of polymorphic structure were also discovered. The sizes of these formations varied from 12.6 to 493.7 μm (Figure 1A).

Histochemistry

Von Kossa staining reflects the presence of calcium phosphate salts. Psammoma bodies and their fragments in the tumor tissue are colored black and dark brown (Figure 1B). In psammoma bodies is noted the boundaries of the layers are visualized and the difference in color saturation between the core and the shell of the formation.

Immunohistochemistry

Immunohistochemical examination of the tissue of ovarian serous carcinomas with antibodies against OPN showed the accumulation of this

protein on the surface of biomineral formations (Figure 1C). The protein covers the surface of the calcification, accumulating at the edges of the formation and between the lamellae of the PBs. A positive cytoplasmic reaction to OPN is also observed in the cells of the tumor microenvironment. Mostly mononuclear and fibroblast-like morphology. Based on this, we can talk about the presence of hydroxyapatite in the structural composition of PBs. Accumulation of OC was visualized on the surface of lamellar structures with a significantly higher intensity at the periphery, which indicates the content of a protein component in the structure of PBs (Figure 1D).
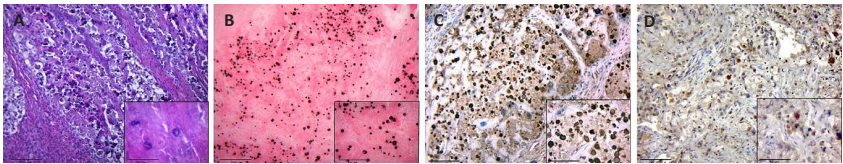
**Figure 1. Pathological biominerals of ovarian cancer.
(A) staining with hematoxylin-eosin; (B) von Kossa staining;
Immunostaining with (C) Anti-Osteopontin Antibody (OPN)
and (D) Anti-Amyloid Fibrils OC Antibody (OC)**

Morphometric analysis

Analysis of images of histological examination demonstrates the presence of PBs in tumor tissue of the ovary. Their number varied from 1 to 200 units. PBs were mainly localized at the base of papillary growths of ovarian serous carcinoma and tumor tissue detritus. A significant amount of PBs was located in the thickness of the connective tissue of the tumor nodes, as well as in the adjacent intact tissue of the ovaries. Remnants of vascular walls of capillaries were found around PBs. PBs had a lamellar structure and were often presented in the form of fragments and fragments that preserved the primary structure of the biomineral.

Analysis of morphometric characteristics of PBs based on images of histological and immunohistochemical methods of research showed fluctuations in the size of PBs from 12.6 to 493.7 μm. According to their structure, PBs consists of lamellae and lamellar layers, which are arranged in sequential order. This sequence may indicate the cyclic nature of PBs formation processes. The average thickness of the lamellar layer was 3.7 μm

($\pm$ 0.17), and the average thickness of the lamellae was 0.65 μm ($\pm$ 0.02). It was established that the thickness of the lamellar layer has a direct strong correlation with the size of PBs ($r = 0.79$; $p < 0.001$), which may indicate the staged formation of these bodies. At the same time, the thickness of the lamellae has a very weak correlation with the dimensions of the PT ($r = 0.1$; $p > 0.05$). The thickness of lamellae and lamellar layer also has a very weak correlation ($r = 0.08$; $p > 0.05$).

According to the size of PBs, they can be divided into 3 groups: large – more than 200 μm (visualized during ultrasound examination), medium – 71-199 μm and small – up to 70 μm in size.

### *Scanning electron microscopy with EDX*

Scanning electron microscopy (SEM) showed that calcifications are particles of different sizes, and rounded shapes, and have a fragile structure, this is directly confirmed by the presence of fragments of a chimeric configuration. At high magnifications, fractures are characterized by a porous structure of mineral deposits. Spherical and needle-shaped nanocrystalline structures are found on the surface of the calcifications (Figure 2A).

In the EDX spectra, there are main lines of Ca and P, as well as slightly expressed lines of O, C, Mg, Na, and others. The intensity ratio of Ca and P lines reflects the characteristic features of hydroxyapatite $Ca_{10}(PO_4)_6(OH)_2$ (Figure 2B). However, there is a slight difference in the microelement composition shown by the given spectra.
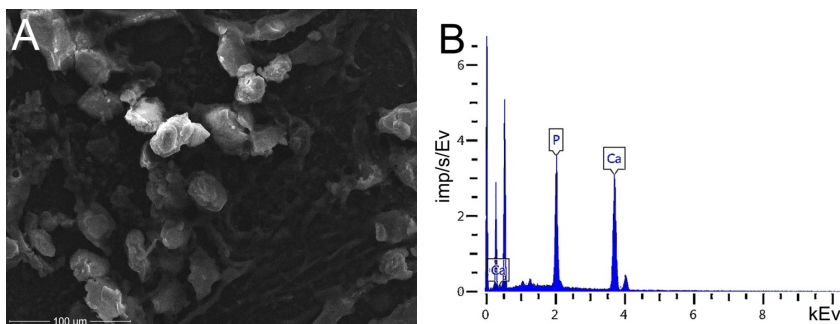
**Figure 2. (A) Scanning electron microscopy (SEM)
with energy-dispersive X-ray spectroscopy (EDX).
(B) EDX spectra of PBs ovarian cancer**

According to the data of the distribution maps of the elements, the accumulation of calcium (Ca), phosphorus (P), and oxygen (O) in the places of localization of calcified particles were established. The distribution density of Ca and P tends to decrease in intensity of accumulation from the center to the periphery, which indicates the different maturity of calcium-phosphate compoundsThere was a uniform distribution of carbon (C) over the field of the scanning sample with no signs of accumulation in the locations of biominerals (shielding by calcification of the carbon-containing surface of the graphite table from the electron beam) (Figure 3).
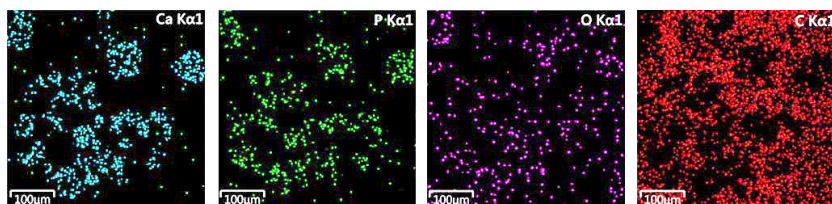

**Figure 3. Study of serous ovarian carcinoma PBs by EDX mapping:
red indicates carbon, purple–oxygen, green–calcium,
blue–phosphorus**

Transmission electron microscopy

Transmission electron microscopy demonstrates the poly- and monodispersity of apatite crystals. The electron diffraction (ED) pattern indicates the polycrystalline nature of these mineral inclusions.

The electron microscopic image shows relatively large crystals (40-50 nm) surrounded by small crystal particles (5-15 nm), which illustrates the polydisperse morphology of nano-sized crystals of the pathological deposit (Figure 4A-B).
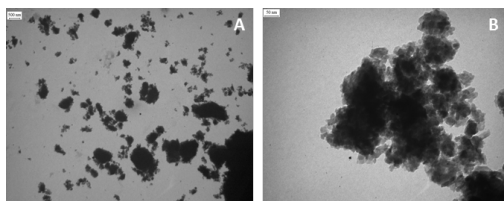
Figure 4. TEM of ovarian cancer with pathological biominerals (A-B)

6. Discussion and conclusions

The calcification process is one of the clinical and morphological features of ovarian tumors. In the case of malignant tumors of the ovaries, the process of pathological biomineralization begins at the earliest stages. This is caused by the partial death of malignant tumor cells, the detritus of which is the basis for the construction of microcalcifications. Thus, this pathological process can be used for early diagnosis of some malignant neoplasms of the ovaries.

Today, several routines and high-tech minimally invasive diagnostic methods are used, such as ultrasound, computed tomography (CT), magnetic resonance imaging (MRI), intravascular ultrasound (IVUS), optical coherence tomography (OCT), and positron emission tomography (PET). Technical progress makes it possible to diagnose smaller and smaller objects. However, these diagnostic methods have different resolutions.

In comparing the results of ultrasound and histological examination, we established that calcifications smaller than 200 μm are not detected using ultrasound methods.

At the same time, it was established that pathological deposits from 1000 μm are detected with the help of CT. IVUS allows for diagnosing calcifications with a resolution of 100-200 μm [74]. And the most high-tech and informative method is OCT, the resolution of which is 10-20 μm. In the study of Shioi et al., it was shown that some biominerals are X-ray negative [74–76].

This depends on the composition of pathological biominerals and the degree of maturity of the biomineral and its structure. The data, established using TEM and electron microdiffraction (ED), demonstrate structural and morphological features of ovarian apatite crystals that are not detected by other methods. Therefore, diagnostic methods based on TEM with ED (or other high-resolution technique) in the future could improve the early diagnosis of malignant tumors with biomineralization.

We established that the main component of pathological biomineral deposits are calcium phosphate compounds. The Ca/P ratio corresponds to the characteristic features of hydroxyapatite. It is known that hydroxyapatite has a direct effect on tumor activity. Able to suppress the proliferation of tumor cells and induce apoptosis [75].

The immunohistochemical study demonstrates the accumulation of OPN on the surface of biomineral deposits. OPN takes part in the mechanism of bone tissue development and pathological biomineralization [76]. By binding to the surface of calcium-phosphate crystallites (for example, hydroxyapatite), OPN inhibits the calcification process, thereby limiting the growth of biominerals [77]. Accordingly, OPN is detected in the localization of calcified particles and is an absolute and early marker of biomineralization processes and the presence of hydroxyapatite. Also, the accumulation of OC on the surface of biomineral inclusions indicates the content of a protein component in the structure of psammoma bodies.

Therefore, the study of the structure, physicochemical, and phase composition of PBs ovarian cancer, and their imaging features is the possible practical application of this pathological phenomenon for the early diagnosis of ovarian cancer and other malignant tumors with biomineralization.

The structural properties of biomineral deposits of tumor tissue make it possible to increase the accuracy of early diagnosis, and the informativeness of the final result at the pre-and postoperative stages, which can improve the prognosis and preserve the quality of life of patients.

References:

1. Fedorenko Z.P., Mykhailovych Yu.I., Hulak L.O. [Cancer in Ukraine, 2018–2019]. *Bulletin of national cancer registry of Ukraine*. 2020; 21: 60–61.

2. Momenimovahed Z., Tiznobaik A., Taheri S., Salehiniya H. Ovarian cancer in the world: epidemiology and risk factors. Int *J Womens Health.* 2019 Apr 30; 11: 287–299. doi: 10.2147/IJWH.S197604

3. McLemore M.R., Miaskowski C., Aouizerat B.E., Chen L.M., Dodd M.J. Epidemiological and genetic factors associated with ovarian cancer. Cancer Nurs. 2009 Jul-Aug; 32(4): 281(8): 289–90. doi: 10.1097/NCC.0b013e31819d30d6

4. Reid B.M., Permuth J.B., Sellers T.A. Epidemiology of ovarian cancer: a review. *Cancer Biol Med.* 2017 Feb; 14(1): 9–32. doi: 10.20892/j.issn.2095-3941.2016.0084

5. La Vecchia C. Ovarian cancer: epidemiology and risk factors. *Eur J Cancer Prev.* 2017 Jan; 26(1): 55–62. doi: 10.1097/CEJ.0000000000000217

6. Cramer D.W. The epidemiology of endometrial and ovarian cancer. *Hematol Oncol Clin North Am.* 2012 Feb; 26(1): 1–12. doi: 10.1016/j.hoc.2011.10.009

7. Arora T., Mullangi S., Lekkala M.R. Ovarian Cancer. [Updated 2022 Jun 5]. In: StatPearls [Internet]. Treasure Island (FL): StatPearls Publishing; 2022 Jan.

8. Lheureux S., Gourley C., Vergote I., Oza A.M. Epithelial ovarian cancer. Lancet. 2019 Mar 23; 393(10177): 1240–1253. doi: 10.1016/S0140-6736(18) 32552-2. PMID: 30910306.

9. Babaier A., Ghatage P. Mucinous Cancer of the Ovary: Overview and Current Status. *Diagnostics (Basel)*. 2020 Jan 19; 10(1): 52. doi: 10.3390/diagnostics10010052. PMID: 31963927; PMCID: PMC7168201.

10. Yoneda A., Lendorf M.E., Couchman J.R., Multhaupt H.A. Breast and ovarian cancers: a survey and possible roles for the cell surface heparan sulfate proteoglycans. *J Histochem Cytochem*. 2012 Jan; 60(1): 9–21.

11. Lengyel E. Ovarian cancer development and metastasis. Am *J Pathol.* 2010 Sep; 177(3): 1053–64.

12. Thomakos N., Diakosavvas M., Machairiotis N., Fasoulakis Z., Zarogoulidis P., Rodolakis A. Rare Distant Metastatic Disease of Ovarian and Peritoneal Carcinomatosis: A Review of the Literature. *Cancers (Basel)*. 2019 Jul; 24; 11(8): 1044.

13. Casagrande J.T., Louie E.W., Pike M.C., Roy S., Ross R.K., Henderson B.E. "Incessant ovulation" and ovarian cancer. *Lancet*. 1979 Jul 28; 2(8135): 170–3. doi: 10.1016/s0140-6736(79)91435-1. PMID: 89281.

14. Wen J., Miao Y., Wang S., Tong R., Zhao Z., Wu J. Calcification: A Disregarded or Ignored Issue in the Gynecologic Tumor Microenvironments. Int *J Gynecol Cancer*. 2018 Mar; 28(3): 486–492.

15. Pal T., Permuth-Wey J., Betts J.A., Krischer J.P., Fiorica J., Arango H., LaPolla J., Hoffman M., Martino M.A., Wakeley K., Wilbanks G., Nicosia S., Cantor A., Sutphen R. BRCA1 BRCA2 mutations account for a large proportion of ovarian carcinoma cases. *Cancer*. 2005; 104(12): 2807–2816.

16. King M.C., Marks J.H., Mandell J.B. and New York Breast Cancer Study. Breast and ovarian cancer risks due to inherited mutations in BRCA1 and BRCA2. *Science*. 2003; 302(5645): 643–646.

17. Dilley J., Burnell M., Gentry-Maharaj A., Ryan A., Neophytou C., Apostolidou S., Karpinskyj C., Kalsi J., Mould T., Woolas R., Singh N., Widschwendter M., Fallowfield L., Campbell S., Skates S.J., McGuire A., Parmar M., Jacobs I., Menon U. Ovarian cancer symptoms, routes to diagnosis and survival – Population cohort study in the 'no screen' arm of the UK Collaborative Trial of Ovarian Cancer Screening (UKCTOCS). *Gynecol Oncol.* 2020 Aug; 158(2): 316–322. doi: 10.1016/j.ygyno.2020.05.002. Epub 2020 Jun 17. PMID: 32561125; PMCID: PMC7453382.

18. Booth M., Beral V., Smith P. Risk factors for ovarian cancer: a case-control study. *Br J Cancer*. 1989 Oct; 60(4): 592–8. doi: 10.1038/bjc.1989.320. PMID: 2679848; PMCID: PMC2247100.], [Shu X.O., Brinton L.A., Gao Y.T., Yuan J.M. Population-based case-control study of ovarian cancer in Shanghai. *Cancer Res*. 1989 Jul 1; 49(13): 3670-4. PMID: 2731180.

19. Whittemore A.S., Harris R., Itnyre J. Characteristics relating to ovarian cancer risk: collaborative analysis of 12 US case-control studies. II. Invasive epithelial ovarian cancers in white women. Collaborative Ovarian Cancer Group. Am *J Epidemiol.* 1992 Nov 15; 136(10): 1184–203. doi: 10.1093/oxfordjournals.aje.a116427. PMID: 1476141.

20. Kvåle G., Heuch I., Nilssen S., Beral V. Reproductive factors and risk of ovarian cancer: a prospective study. Int *J Cancer.* 1988 Aug 15; 42(2): 246–51. doi: 10.1002/ijc.2910420217. PMID: 3403067.

21. Adami H.O., Hsieh C.C., Lambe M., Trichopoulos D., Leon D., Persson I., Ekbom A., Janson P.O. Parity, age at first childbirth, and risk of ovarian cancer. *Lancet*. 1994 Nov 5; 344(8932): 1250–4. doi: 10.1016/s01406736(94) 90749-8. PMID: 7967985.

22. Chan J.K., Tian C., Kesterson J.P., Monk B.J., Kapp D.S., Davidson B., Robertson S., Copeland L.J., Walker J.L., Wenham R.M., Casablanca Y., Spirtos N.M., Tewari K.S., Bell J.G. Symptoms of Women With High-Risk Early-Stage Ovarian Cancer. *Obstet Gynecol*. 2022 Feb 1; 139(2): 157–162. doi: 10.1097/ AOG.0000000000004642. PMID: 34991145; PMCID: PMC9126568.

23. Huepenbecker S.P., Sun C.C., Fu S., Zhao H., Primm K., Giordano S.H., Meyer L.A. Factors impacting the time to ovarian cancer diagnosis based on classic symptom presentation in the United States. *Cancer*. 2021 Nov 15; 127(22): 4151–4160. doi: 10.1002/cncr.33829. Epub 2021 Aug 4. PMID: 34347287; PMCID: PMC8556293.

24. Lawson-Michod K.A., Watt M.H., Grieshober L., Green S.E., Karabegovic L., Derzon S., Owens M., McCarty R.D., Doherty J.A., Barnard M.E. Pathways to ovarian cancer diagnosis: a qualitative study. *BMC Womens Health*. 2022 Nov 4; 22(1): 430. doi: 10.1186/s12905-022-02016-1. PMID: 36333689; PMCID: PMC9636716.

25. Matulonis U.A. Ovarian Cancer. *Hematol Oncol Clin North Am*. 2018 Dec; 32(6): xiii–xiv. doi: 10.1016/j.hoc.2018.09.006. Epub 2018 Sep 25. PMID: 30390771.

26. Mitra A.K. Ovarian Cancer Metastasis: A Unique Mechanism of Dissemination. *Tumor Metastasis* [Internet]. 2016 Sep 14; DOI: http: //dx.doi.org/ 10.5772/64700

27. Matulonis U.A., Sood A.K., Fallowfield L., Howitt B.E., Sehouli J., Karlan B.Y. Ovarian cancer. *Nat Rev Dis Primers*. 2016 Aug 25; 2: 16061. doi: 10.1038/nrdp.2016.61. PMID: 27558151; PMCID: PMC7290868.

28. Yousefi M., Dehghani S., Nosrati R., Ghanei M., Salmaninejad A., Rajaie S., Hasanzadeh M., Pasdar A. Current insights into the metastasis of epithelial ovarian cancer – hopes and hurdles. *Cell Oncol (Dordr)*. 2020 Aug; 43(4): 515–538. doi: 10.1007/s13402-020-00513-9. Epub 2020 May 16. PMID: 32418122.

29. Lengyel E. Ovarian cancer development and metastasis. Am *J Pathol*. 2010 Sep; 177(3): 1053–64. doi: 10.2353/ajpath.2010.100105. Epub 2010 Jul 22. PMID: 20651229; PMCID: PMC2928939.

30. Cook L.M., Hurst D.R., Welch D.R. Metastasis suppressors and the tumor microenvironment. *Semin Cancer Biol*. 2011 Apr; 21(2): 113–22. doi: 10.1016/j.semcancer.2010.12.005. Epub 2010 Dec 17. PMID: 21168504; PMCID: PMC3053584.

31. Cai J., Tang H., Xu L., Wang X., Yang C., Ruan S., Guo J., Hu S., Wang Z. Fibroblasts in omentum activated by tumor cells promote ovarian cancer growth, adhesion and invasiveness. *Carcinogenesis*. 2012 Jan; 33(1): 20–9. doi: 10.1093/carcin/bgr230. Epub 2011 Oct 21. PMID: 22021907.

32. Yeung T.L., Leung C.S., Yip K.P., Au Yeung C.L., Wong S.T., Mok S.C. Cellular and molecular processes in ovarian cancer metastasis. A Review in the

Theme: Cell and Molecular Processes in Cancer Metastasis. Am *J Physiol Cell Physiol*. 2015 Oct 1; 309(7): C444–56. doi: 10.1152/ajpcell.00188.2015. Epub 2015 Jul 29. PMID: 26224579; PMCID: PMC4593771.

33. Zhang Y., Tang H., Cai J., Zhang T., Guo J., Feng D., Wang Z. Ovarian cancer-associated fibroblasts contribute to epithelial ovarian carcinoma metastasis by promoting angiogenesis, lymphangiogenesis and tumor cell invasion. *Cancer Lett.* 2011 Apr 1; 303(1): 47–55. doi: 10.1016/j.canlet.2011.01.011. PMID: 21310528.

34. Kajiyama H., Suzuki S., Utsumi F., Nishino K., Niimi K., Mizuno M., Yoshikawa N., Kawai M., Oguchi H., Mizuno K., Yamamuro O., Shibata K., Nagasaka T., Kikkawa F. Epidemiological overview of metastatic ovarian carcinoma: long-term experience of TOTSG database. *Nagoya J Med Sci.* 2019 May; 81(2): 193–198. doi: 10.18999/nagjms.81.2.193. PMID: 31239587; PMCID: PMC6556446.

35. Nakayama K., Nakayama N., Katagiri H., Miyazaki K. Mechanisms of ovarian cancer metastasis: biochemical pathways. Int *J Mol Sci.* 2012; 13(9): 11705–11717. doi: 10.3390/ijms130911705. Epub 2012 Sep 18. PMID: 23109879; PMCID: PMC3472771.

36. Slomovitz B., Gourley C., Carey M.S., Malpica A., Shih I.M., Huntsman D., Fader A.N., Grisham R.N., Schlumbrecht M., Sun C.C., Ludemann J., Cooney G.A., Coleman R., Sood A.K., Mahdi H., Wong K.K., Covens A., O'Malley D.M., Lecuru F., Cobb L.P., Caputo T.A., May T., Huang M., Siemon J., Fernández M.L., Ray-Coquard I., Gershenson D.M. Low-grade serous ovarian cancer: State of the science. *Gynecol Oncol*. 2020 Mar; 156(3): 715–725. doi: 10.1016/j.ygyno.2019.12.033. Epub 2020 Jan 20. PMID: 31969252.

37. Nougaret S., Lakhman Y., Molinari N., Feier D., Scelzo C., Vargas H.A., Sosa R.E., Hricak H., Soslow R.A., Grisham R.N., Sala E. CT Features of Ovarian Tumors: Defining Key Differences Between Serous Borderline Tumors and Low-Grade Serous Carcinomas. *AJR Am J Roentgenol*. 2018 Apr; 210(4): 918–926. doi: 10.2214/AJR.17.18254. Epub 2018 Feb 28. PMID: 29489407; PMCID: PMC6690180.

38. Chyzhma R., Piddubnyi A., Danilchenko S., Kravtsova O., Moskalenko R. Potential Role of Hydroxyapatite Nanocrystalline for Early Diagnostics of Ovarian Cancer. *Diagnostics (Basel)*. 2021 Sep 22; 11(10): 1741. doi: 10.3390/diagnostics 11101741. PMID: 34679439; PMCID: PMC8534774.

39. Moskalenko R.A. Biomineralizatsiia u tkanynakh liudskoho orhanizmu. Aktualni problemy suchasnoi medytsyny: *Visnyk ukrainskoi medychnoi stomatolohichnoi akademii*. 2017; 17 (1(57)): 308–313. (in Ukrainian)

40. Murshed M. Mechanism of Bone Mineralization. *Cold Spring Harb Perspect Med.* 2018 Dec 3; 8(12): a031229. doi: 10.1101/cshperspect.a031229. Erratum in: Cold Spring Harb Perspect Med. 2020 Aug 3; 10(8): PMID: 29610149; PMCID: PMC6280711.

41. Das D.K. Psammoma body: a product of dystrophic calcification or of a biologically active process that aims at limiting the growth and spread of tumor? *Diagn Cytopathol*. 2009 Jul; 37(7): 534–41. doi: 10.1002/dc.21081. PMID: 19373908.

42. Bai Y., Zhou G., Nakamura M., Ozaki T., Mori I., Taniguchi E., Miyauchi A., Ito Y., Kakudo K. Survival impact of psammoma body, stromal calcification,

and bone formation in papillary thyroid carcinoma. *Mod Pathol.* 2009 Jul; 22(7): 887-94. doi: 10.1038/modpathol.2009.38. Epub 2009 Mar 20. PMID: 19305382.

43. Elsherif S., Javadi S., Viswanathan C., Faria S., Bhosale P. Low-grade epithelial ovarian cancer: what a radiologist should know. *Br J Radiol.* 2019 Mar; 92(1095): 20180571. doi: 10.1259/bjr.20180571. Epub 2019 Jan 31. PMID: 30604635; PMCID: PMC6541194.

44. Pannu H.K. CT features of low grade serous carcinoma of the ovary. *Eur J Radiol Open.* 2015 Feb 3; 2: 39–45. doi: 10.1016/j.ejro.2015.01.001. PMID: 26937434; PMCID: PMC4750573.

45. Golub E.E. Biomineralization and matrix vesicles in biology and pathology. *Semin Immunopathol.* 2011 Sep; 33(5): 409–17. doi: 10.1007/s00281-010-0230-z. Epub 2010 Dec 8. PMID: 21140263; PMCID: PMC3139768.

46. Murshed M., McKee M.D. Molecular determinants of extracellular matrix mineralization in bone and blood vessels. *Curr Opin Nephrol Hypertens.* 2010 Jul; 19(4): 359–65. doi: 10.1097/MNH.0b013e3283393a2b. PMID: 20489614.

47. Ito S., Saito T., Amano K. In vitro apatite induction by osteopontin: interfacial energy for hydroxyapatite nucleation on osteopontin. *J Biomed Mater Res A.* 2004 Apr 1; 69(1): 11–6. doi: 10.1002/jbm.a.20066. PMID: 14999746.

48. Harmey D., Hessle L., Narisawa S., Johnson K.A., Terkeltaub R., Millán J.L. Concerted regulation of inorganic pyrophosphate and osteopontin by akp2, enpp1, and ank: an integrated model of the pathogenesis of mineralization disorders. Am *J Pathol.* 2004 Apr; 164(4): 1199–209. doi: 10.1016/S0002-9440(10)63208-7. PMID: 15039209; PMCID: PMC1615351.

49. Dean D.D., Schwartz Z., Muniz O.E., Gomez R., Swain L.D., Howell D.S., Boyan B.D. Matrix vesicles are enriched in metalloproteinases that degrade proteoglycans. *Calcif Tissue Int.* 1992 Apr; 50(4): 342–9. doi: 10.1007/BF00301632. PMID: 1571846.

50. Anderson H.C. Mechanisms of pathologic calcification. *Rheum Dis Clin North Am.* 1988 Aug; 14(2): 303–19. PMID: 2845491.

51. Vimalraj S. Alkaline phosphatase: Structure, expression and its function in bone mineralization. *Gene*. 2020 Sep 5; 754: 144855. doi: 10.1016/j.gene.2020.144855. Epub 2020 Jun 6. PMID: 32522695.

52. Amadeu de Oliveira F., Narisawa S., Bottini M., Millán J.L. Visualization of Mineral-Targeted Alkaline Phosphatase Binding to Sites of Calcification In Vivo. *J Bone Miner Res*. 2020 Sep; 35(9): 1765–1771. doi: 10.1002/jbmr.4038. Epub 2020 May 8. PMID: 32343017; PMCID: PMC8383212.

53. Ganeshan D., Bhosale P., Wei W. Increase in post-therapy tumor calcification on CT scan is not an indicator of response to therapy in low-grade serous ovarian cancer. *Abdom Radiol (NY)*. 2016; 41(8): 1589–95.

54. Fanl M., Changqiu W., Yan L. Psammoma bodies in two types of human ovarian tumours: a mineralogical study. *Miner Petrol.* 2015; 109: 357–65.

55. Silva E.G., Deavers M.T., Parlow A.F., Gershenson D.M., Malpica A. Calcifications in ovary and endometrium and their neoplasms. *Mod Pathol.* 2003 Mar; 16(3): 219–22.

56. Okada S., Ohaki Y., Inoue K., Kawamura T., Hayashi T., Kato T., Kumazaki T. Calcifications in mucinous and serous cystic ovarian tumors. *J Nippon Med Sch.* 2005 Feb; 72(1): 29–33.

57. Hudelist G., Singer C.F., Kubista E., Manavi M., Mueller R., Pischinger K., Czerwenka K. Presence of nanobacteria in psammoma bodies of ovarian cancer: evidence for pathogenetic role in intratumoral biomineralization. *Histopathology.* 2004 Dec; 45(6): 633–7.

58. Wen J., Zhao Z., Huang L., Li L., Li J., Zeng Y., Wu J., Miao Y. Switch of the ovarian cancer cell to a calcifying phenotype in the calcification of ovarian cancer. *J Cancer.* 2018 Feb 28; 9(6): 1006–1016.

59. Hale E.K. Metastatic calcification. *Dermatol Online J.* 2003 Oct; 9(4): 2. PMID: 14594575.

60. Burkill G.J., Allen S.D., A'hern R.P., Gore M.E., King D.M. Significance of tumour calcification in ovarian carcinoma. *Br J Radiol.* 2009 Aug; 82(980): 640–4. doi: 10.1259/bjr/12716831. Epub 2009 Mar 30. PMID: 19332521.

61. Vidavsky N., Kunitake J.A.M.R., Estroff L.A. Multiple Pathways for Pathological Calcification in the Human Body. *Adv Healthc Mater.* 2021 Feb; 10(4): e2001271. doi: 10.1002/adhm.202001271. Epub 2020 Dec 4. PMID: 33274854; PMCID: PMC8724004.

62. Lee S.J., Lee I.K., Jeon J.H. Vascular Calcification-New Insights Into Its Mechanism. Int *J Mol Sci.* 2020 Apr 13; 21(8): 2685. doi: 10.3390/ijms21082685. PMID: 32294899; PMCID: PMC7216228.

63. Fukumoto S. [Ectopic calcification]. *Clin Calcium.* 2014 Feb; 24(2): 185–9. Japanese. PMID: 24473351.

64. Olivera Merlin P.S., Leyva Bohorquez Pdel C., Martínez-Cruz R., Pina Canseco S., Hernandez P., Martínez-Cruz M., et al. A study on inorganic elements in psammomas from ovarian & thyroid cancer. *Indian J Med Res.* 2012; 135(2): 217–20.

65. Iline-Vul T., Nanda R., Mateos B., Hazan S., Matlahov I., Perelshtein I., Keinan-Adamsky K., Althoff-Ospelt G., Konrat R., Goobes G. Osteopontin regulates biomimetic calcium phosphate crystallization from disordered mineral layers covering apatite crystallites. *Sci Rep.* 2020 Sep 24; 10(1): 15722. doi: 10.1038/s41598-020-72786-x. PMID: 32973201; PMCID: PMC7518277.

66. Zhao H., Chen Q., Alam A., Cui J., Suen K.C., Soo A.P., et al. The role of osteopontin in the progression of solid organ tumour. *Cell Death Dis.* 2018 Mar 2; 9(3): 356.

67. Wang Z.Q., Keita M., Bachvarova M., Gobeil S., Morin C., Plante M., et al. Inhibition of RUNX2 transcriptional activity blocks the proliferation, migration and invasion of epithelial ovarian carcinoma cells. *PLoS One.* 2013 Oct 4; 8(10): e74384.

68. Condello S., Morgan C.A., Nagdas S., Cao L., Turek J., Hurley T.D., Matei D. β-Catenin-regulated ALDH1A1 is a target in ovarian cancer spheroids. *Oncogene.* 2015 Apr 30; 34(18): 2297–308.

69. Qian J., LeSavage B.L., Hubka K.M., Ma C., Natarajan S., Eggold J.T., Xiao Y., Fuh K.C., Krishnan V., Enejder A., Heilshorn S.C., Dorigo O., Rankin E.B. Cancer-associated mesothelial cells promote ovarian cancer chemoresistance through paracrine osteopontin signaling. *J Clin Invest.* 2021 Aug 16; 131(16): e146186. doi: 10.1172/JCI146186. PMID: 34396988; PMCID: PMC8363279.

70. Cerne K., Hadzialjevic B., Skof E., Verdenik I., Kobal B. Potential of osteopontin in the management of epithelial ovarian cancer. *Radiol Oncol.* 2019 Jan 31; 53(1): 105–115. doi: 10.2478/raon-2019-0003. PMID: 30712025; PMCID: PMC6411016.

71. Li N., Wang L., Tan G., Guo Z., Liu L., Yang M., He J. Retraction: MicroRNA-218 inhibits proliferation and invasion in ovarian cancer by targeting Runx2. *Oncotarget.* 2022 Jul 2; 13: 863. doi: 10.18632/oncotarget.28253. PMID: 35813282; PMCID: PMC9255994.

72. Brum M.C.M., Dos Santos Guimaraes I., Ferreira L.B., Rangel L.B.A., Maia R.C., Nestal De Moraes G., Gimba E.R.P. Osteopontin-c isoform inhibition modulates ovarian cancer cell cisplatin resistance, viability and plasticity. *Oncol Rep.* 2021 Feb; 45(2): 652–664. doi: 10.3892/or.2020.7877. Epub 2020 Dec 1. PMID: 33416171; PMCID: PMC7757104.

73. Wen C., Liu X., Ma H., Zhang W., Li H. [Retracted] miR-338-3p suppresses tumor growth of ovarian epithelial carcinoma by targeting Runx2. Int *J Oncol.* 2021 Aug; 59(2): 57. doi: 10.3892/ijo.2021.5237. Epub 2021 Jul 1. PMID: 34195848; PMCID: PMC8253587.

74. Shioi A., Ikari Y. Plaque Calcification During Atherosclerosis Progression and Regression. *J Atheroscler Thromb.* 2018 Apr 1; 25(4): 294–303. doi: 10.5551/jat.RV17020. Epub 2017 Dec 12. PMID: 29238011; PMCID: PMC5906181.

75. Tang W., Yuan Y., Liu C., Wu Y., Lu X., Qian J. Differential cytotoxicity and particle action of hydroxyapatite nanoparticles in human cancer cells. *Nanomedicine (Lond).* 2014 Mar; 9(3): 397-412. doi: 10.2217/nnm.12.217. Epub 2013 Apr 24. PMID: 23614636.

76. Maki M., Hirota S., Kaneko Y., Morohoshi T. Expression of osteopontin messenger RNA by macrophages in ovarian serous papillary cystadenocarcinoma: a possible association with calcification of psammoma bodies. *Pathol Int.* 2000 Jul; 50(7): 531–5. doi: 10.1046/j.1440-1827.2000.01075.x. PMID: 10886734.

77. Hunter G.K. Role of osteopontin in modulation of hydroxyapatite formation. *Calcif Tissue Int.* 2013 Oct; 93(4): 348–54. doi: 10.1007/s00223-013-9698-6. Epub 2013 Jan 19. PMID : 23334303.